Preferred citation: K. Oh, M. Lee, H.J. Youn, D.H. Jeong and H.L. Lee. Paper-based chemical detecting sensors for surface-enhanced Raman scattering. In **Advances in Pulp and Paper Research, Oxford 2017**, *Trans. of the XVIth Fund. Res. Symp. Oxford, 2017*, (W. Batchelor and D. Söderberg, eds), pp 751–773, FRC, Manchester, 2018. DOI: 10.15376/frc.2017.2.751.

PAPER-BASED CHEMICAL DETECTING SENSORS FOR SURFACE-ENHANCED RAMAN SCATTERING

*Kyudeok Oh[1,2], Minwoo Lee[3], Hye Jung Youn[1,2], Dae Hong Jeong[3] and Hak Lae Lee[1,2]**

[1] Department of Forest Sciences, College of Agriculture and Life Sciences
[2] Research Institute of Agriculture and Life Sciences, Seoul National University
[3] Department of Chemistry Educations, College of Education, Seoul National University

ABSTRACT

In this study, we fabricated a paper-based molecule-detecting sensor for the surface-enhanced Raman scattering (SERS) technique. SERS phenomenon is based on the fact that the low intensity of Raman scattering is dramatically increased when the molecules are adsorbed on novel metal surface. To improve the applicability of paper substrate as a base for SERS several trials were made. The smoothness of the filter paper was improved through a calendaring process. To prevent the spreading of the chemical solution on the paper the hydrophobicity of paper was increased by treating with an alkyl ketene dimer (AKD). Onto the smooth and hydrophobic filter paper a silver nanoparticle (AgNP) solution was applied with a simple drop and dry method, and the analyte was treated in the same manner on the AgNP decorated area for SERS measurement. To improve the reproducibility of the SERS intensity, an area scanning method that used a dual axis galvanometric mirror was introduced. A 4-aminothiophenol molecule could be detected at the femtomolar level using the hydrophobic-treated filter paper. Coatings of cellulose nanofibrils (CNF) made

* Corresponding author: lhakl@snu.ac.kr

from pulp fibres reduced the surface pore sizes and increased the uniformity of the surface of the filter paper, which improved the reproducibility and sensitivity of the molecule-detecting sensor. The use of a high magnification objective lens for increased SERS intensity allowed for the detection of a strong SERS signal, and the application of a CNF coating to the filter paper improved the reproducibility. Pesticides were detected using the paper-based substrate as the SERS substrate.

Keywords: Surface-enhanced Raman scattering (SERS), filter paper, cellulose nanofibrils (CNF), silver nanoparticle (AgNP), sensor

1 INTRODUCTION

Surface-enhanced Raman scattering (SERS) is a technique to enhance Raman scattering using metallic nanoparticles that adsorb molecules to analyse. Since the introduction of SERS by Fleischmann in the 1970s, many researchers have tried applying SERS phenomena to various fields. Scientists have been very interested in detecting molecules using the advantages of the SERS technique, which include a sensitive signal, unique molecular spectra and a narrow bandwidth of spectra. However, the SERS technique can be disadvantageous for use as a molecule-detection sensor because of the large variation in the sensitivity and uniformity of the signal depending on the state of the novel metal surface.

To overcome these disadvantages, many studies have been carried out to introduce a uniform metal nanoarray on the solid substrate surface. These studies have used substrates such as polydimethylacrylamide (PDMA), slide glass and silicon using electrochemical deposition [1]–[3], vapour deposition [4], [5], electron beam lithography [6], [7] or colloidal lithography [8], [9]. The generated substrates have shown high sensitivity and reproducibility of the SERS signal, but the preparation of such substrates required complicated processes or machines and had high costs. These substrates are therefore being made in the laboratory.

Many researchers have worked on devising a paper-based SERS substrate as an alternative to conventional SERS substrate fabrication methods. The filter paper substrate has been favoured as a substitute for the conventional SERS substrate because it is inexpensive, has a high biodegradability, is easy to handle and functionalise and has good disposability. However, due to the hydrophilic nature of the filter paper and the presence of large pores, the retention of nanoparticles on the surface was limited. The roughness of the filter paper can also cause an uneven distribution of the novel metal particles, resulting in a non-uniform SERS signal.

Many methods such as adsorption [10]–[14], aggregation of nanoparticles [15], nanoparticle filtering [16], printing [17], [18], chemical reaction on the filter paper [19]–[23] and vapour deposition [26] have been used to deposit nanoparticles on the filter paper. These methods can face problems in fabricating a SERS hot spot from the aggregation of nanoparticles, non-uniform SERS intensity, shape control of nanoparticles and the high cost.

We aimed to overcome the challenges described in previous studies by inducing hydrophobicity in the filter paper to increase the retention of nanoparticles on the paper surface and by improving surface smoothness through filling the paper pores with cellulose nanofibrils (CNF) that originated from pulp fibres. We tested how these two modifications of the filter paper affected the detection of trace amounts of a molecule. The drop and dry method was used to form the SERS active spot on the filter paper and additional drop and dry applications of analyte were applied to ensure that the analyte was adsorbed on the metal surface.

2 EXPERIMENTAL

2.1 Materials and reagents

Silver nitrate ($AgNO_3$, 99.999%), sodium citrate dehydrate ($Na_2HC_6H_5O_7$, 99%), 4-aminothiophenol (4-ATP, 99%) were purchased from Sigma-Aldrich (St. Louis, MO, USA). Filter paper (grade 5C) was purchased from Advantec (Tokyo, Japan), and the alkylketene dimer (AKD) was Hercon-WI 155, which was purchased from Solenis, Korea Ltd (Kimchun, Korea). All chemicals were used without further purification.

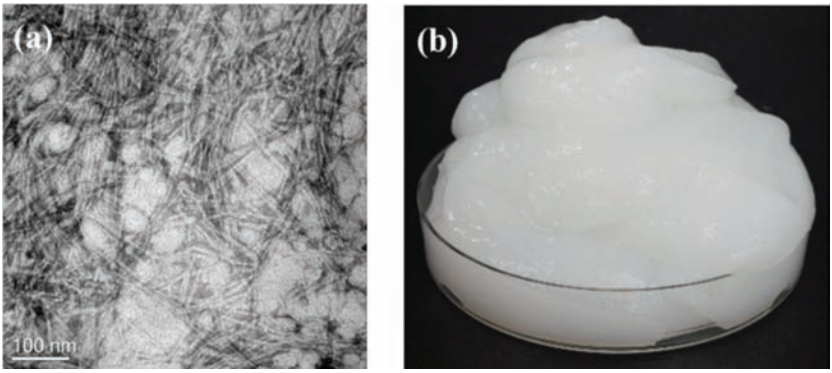

Figure 1. (a): TEM image of CNF. (b): CNF gel (solids content: 2.2%).

The CNF was prepared by grinding bleached eucalyptus kraft pulp with a grinder (Super Masscolloider, Masuko Co.). Before the grinding, the bleached eucalyptus kraft pulp was pretreated by a laboratory Valley beater. The Canadian Standard Freeness (CSF) of the pulp was 450 mL. TEM image of the CNF is shown in Figure 1(a). The widths of CNF were less than 50 nm. The pass number for preparation of CNF was more than 30 (CNF gel in Figure 1(b)). Carboxymethyl cellulose (DS 0.78; CMC; Finnfix 5, CP Kelco Korea) was used to control the rheological properties of the CNF suspension.

2.2 Silver nanoparticle synthesis and characteristics

Silver nanoparticles (AgNPs) were synthesised using methods modified from Lee and Meisel [29]. Briefly, 75 mg of silver nitrate was dissolved in 400 mL of deionised water in a 3-neck round bottom flask with vigorous stirring. After the silver

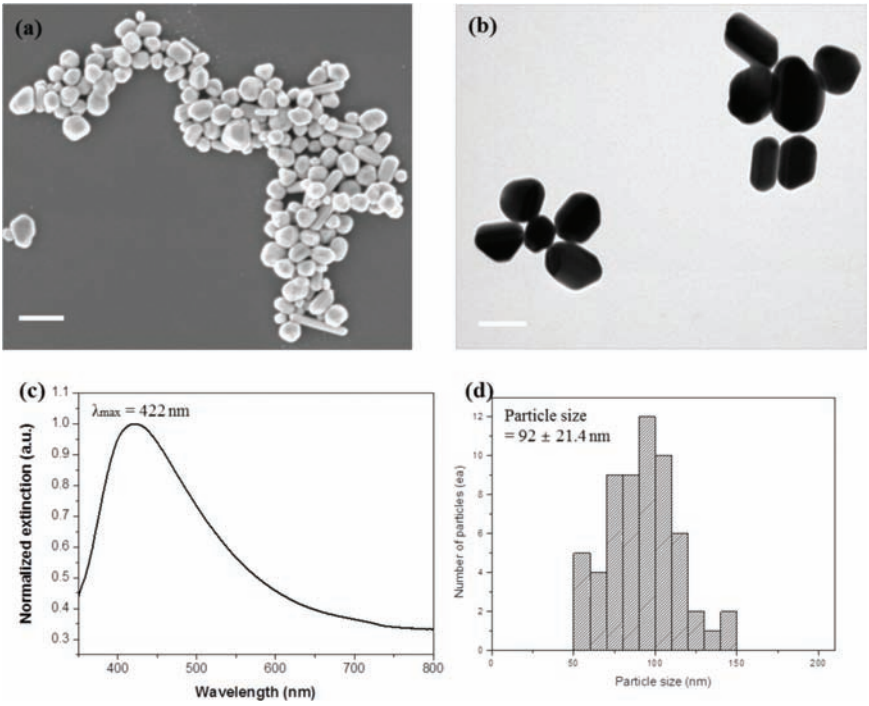

Figure 2. Characterisation of the AgNPs. (a) FE-SEM and (b) TEM images of AgNP. (c) UV-Vis spectrum of AgNP. (d) Size distribution of 100 AgNPs measured from SEM images. Scale bars are 100 nm.

nitrate solution was boiled, 8 mL of 1wt% sodium citrate in deionised water was rapidly injected into the 3-neck round bottom flask. The solution was heated for 30 min and then was cooled at room temperature.

The particle shape was characterised by viewing with a field emission scanning electron microscope (FE-SEM, AURIGA, Carl Zeiss, Germany) and transmission electron microscope (TEM, LIBRA 120, Carl Zeiss, Germany). UV/Vis spectra were also collected. The shapes of the AgNPs are shown in Figure 2(a) and 2(b). The UV-Vis extinction spectra of the AgNPs showed a maximum peak at 422 nm. The average size of the AgNPs in the FE-SEM images was about 92 nm.

2.3 Hydrophobic filter paper fabrication

A schematic illustration of the hydrophobic filter paper fabrication is shown in Figure 5. To reduce the roughness of the filter paper, a calendaring process was used in which the filter paper passed in-between rotating rolls. The rotating speed, calendaring temperature, relative humidity (RH), and line pressure were 10 m/min, 23 °C, RH 50%, and 130 kgf/cm, respectively. After the calendaring of filter paper, the alkylketene dimer (AKD) was used as a hydrophobic agent to increase the hydrophobicity of the filter paper. The calendared filter paper was soaked in a 0.1% AKD dispersion for 1 min. After the AKD treatment, the filter paper was rinsed thoroughly with water. Water that remained in the treated filter paper was eliminated using another filter paper (Filter paper 26, Advantec, Japan) and the treated filter paper was then dried using a drum drier at 120 °C.

2.4 CNF coating

To improve paper-based SERS substrates, CNF suspension containing a small amount of CMC was applied. The total solids content of the suspension was 1wt%, and the CMC content was 3 pph based on dried CNF. The prepared CNF suspension was applied onto the hydrophobic-treated filter paper with a laboratory bar coater (GIST, Korea). The coating was applied up to two times using a rod (No. 14). The coated paper was then dried using a hot air dryer (120 °C, 150 sec). After the CNF coating, the AKD treatment was conducted to introduce a uniform hydrophobic surface. The procedures for AKD treatment and drying were same as described in section 2.3.

2.5 Characterisation of the filter paper-based substrate

The roughness of the filter paper was evaluated using a Parker Print Surf (PPS, L&W, Sweden) instrument (ISO 8791-4). The measurement pressure was 1 MPa.

The contact angle of water was measured using a contact angle meter (DSA100, Kruss, Germany) after forming a 5 μL water drop on the surface.

2.6 SERS-active AgNP array fabrication

For fabrication of a SERS-active array on hydrophobic filter paper, 2 μL of the AgNP solution was applied using the drop and dry method at room temperature for about 1 h. After the AgNP solution dried, 5 μL of each analyte solution was applied using the drop and dry method on the AgNP array. We covered the entire area of the AgNP spot for the SERS measurement. The photograph of the AgNP array on the filter paper is shown in Figure 3. The spot area was much larger than that of the hydrophobic-treated filter paper. Deeper colour was noted on the hydrophobic filter paper because more of the AgNPs remained on the surface of the filter paper.

2.7 SERS measurements

SERS spectra were acquired by a hand-made Raman read-out system for a large-area scanning. A 643-nm laser line (115-81040-019, Ondax, US) was used for the Raman excitation source. The laser line was delivered through a dual axis galvanometric mirror for an area scanning centred on the AgNP spot. An objective lens (Olympus, Japan) was used at different magnifications and numerical apertures (NA) for the collection of irradiated and scattered light. The magnifications and NAs were: 10× (NA = 0.25), 20× (NA = 0.40) and 40× (NA = 0.65). The scattered light was read by a charge-coupled device (iDus 416, Andor, UK).

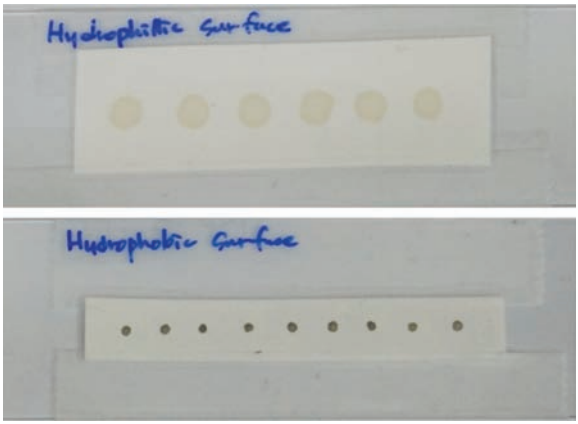

Figure 3. AgNP array on bare (hydrophilic) filter paper and hydrophobic filter paper.

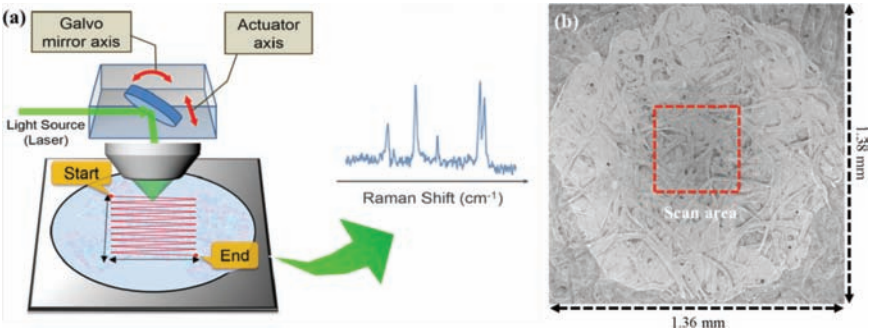

Figure 4. (a) Schematic of the SERS measurement from a large-area scanning system [24]. (b) Scanning area in the AgNP spot.

3 RESULTS AND DISCUSSION

3.1 Hydrophobic treatment

3.1.1 Schematics and characterisation of filter paper

Figure 5(a) shows a schematic of the surface treatment process. The hydrophobic surface was introduced to prevent penetration of the AgNPs and analyte into the filter paper. The hydrophobicity of the filter paper was confirmed by the measurement of the contact angle. The contact angle of the bare filter paper was 15 °; however, it was increased up to 114 ° after the AKD treatment (Figure 5(b) and 5(c)). Thus, we confirmed that the droplet of AgNP solution and analyte formed on the surface of the paper.

The roughness of the filter paper, shown in Figure 6, was decreased from 9.4 μm to 4.0 μm by the calendaring procedure. The simple physical treatment of calendaring can reduce the roughness of the filter paper by about 40%. The roughness of the filter paper was increased up to 5.7 μm after the AKD treatment because the cellulose fibres swelled during the treatment.

The distributions of the AgNPs before and after AKD treatment were measured by FE-SEM images, as shown in Figure 7(a) and 7(b). In the case of the filter paper before the hydrophobic treatment, the AgNP solution penetrated into the paper, and the AgNPs rarely existed on the surface. For that reason, it was impossible to form a SERS hot spot on the bare filter paper. The AgNP solution was left on the surface of the filter paper after hydrophobic treatment. Thus, an abundance of AgNPs remained on the paper surface and formed the SERS hot spot. To assess the feasibility of the treated filter paper as a SERS substrate, 5 μL of a 1000 nM 4-ATP solution was applied to the filter paper before and after

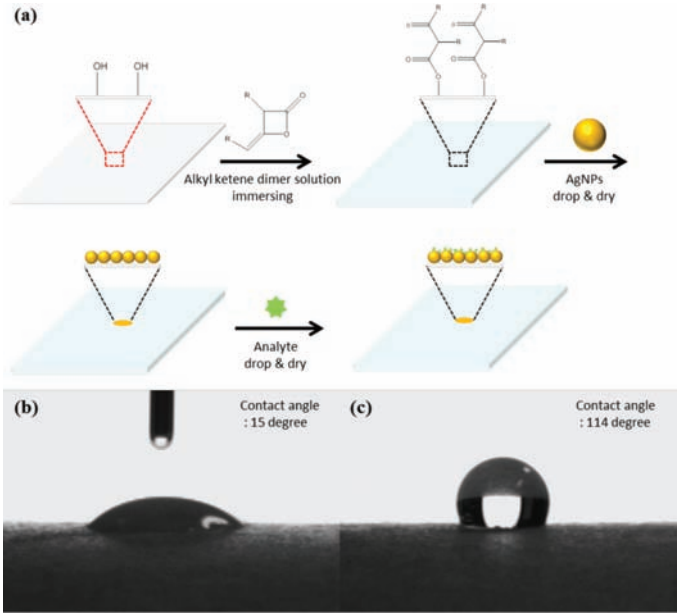

Figure 5. (a) Schematic illustration of the fabrication of the filter paper-based SERS substrate. Photographs of (b) before AKD treatment (bare filter paper), and (c) after AKD treatment (hydrophobic filter paper).

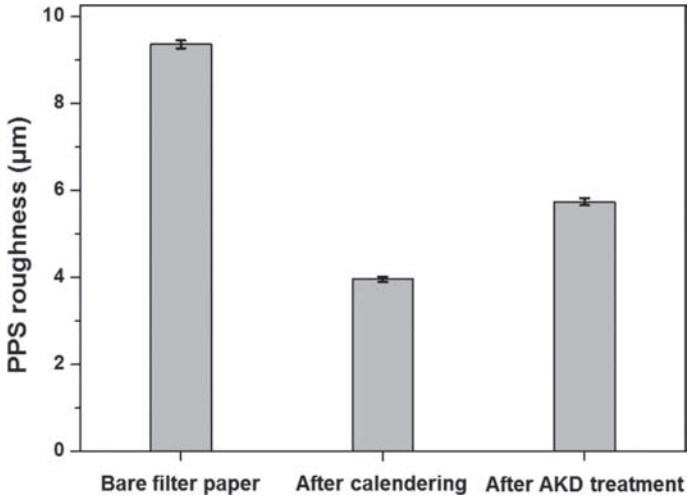

Figure 6. Roughness of the filter paper depended on calendaring and the AKD treatment.

the AKD treatment and SERS measurements were conducted. The scanning size, step size and laser power were 300 μm by 300 μm, 1 μm and 1.5 mW, respectively. An objective lens at 20× magnification was used, and the scanning time was 2.5 sec. The SERS signals did not appear in the bare filter paper; however, there were strong SERS signals measured from the hydrophobic filter paper (Figure 7(c)). In the case of the bare filter paper, the drop of 4-ATP solution soaked into the filter paper quickly, and the molecules were difficult to adsorb onto the surface of the AgNPs. In the case of the hydrophobic-treated filter paper, however, there was enough time for molecules to be adsorbed onto the surface of the AgNPs. Thus, we confirmed that the hydrophobic filter paper was a SERS-active substrate.

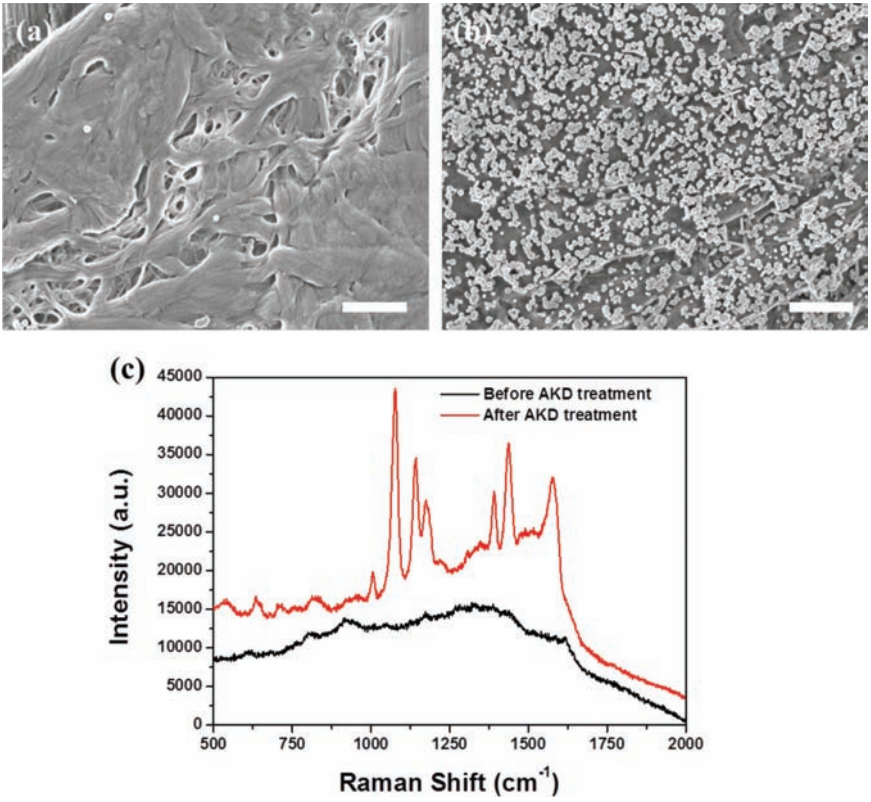

Figure 7. FE-SEM images of the filter paper surface after introduction of 2 μL of a AgNP solution onto the surface (a) before the AKD treatment and (b) after the AKD treatment. (c) SERS spectra of 5 μL of 1,000 nM 4-ATP on the AgNP droplet.

3.1.2 Control of the AgNP distribution for optimisation of SERS intensity

For optimisation of the SERS intensity measured from the SERS-active filter paper, different concentrations of the AgNP solution were applied on the hydrophobic filter paper in addition to 5 μL of 1,000 nM of 4-ATP solution. The more AgNPs that were left on the surface of the filter paper increased the concentration of the AgNP solution (Figure 8(a) to 8(h)). The AgNP solution that was concentrated up to 10× formed the monolayer structure of the AgNPs; however, the AgNP solution that was concentrated over 20× resulted in a multilayer and aggregated structure. The change in the SERS intensity of the 1073 cm^{-1} band of 4-ATP is shown in Figure 9. The SERS intensity of 4-ATP was maximised in the spot that was formed by the 10× concentrated AgNP solution and then the intensity decreased with increasing AgNP solution concentration. As the concentration of the AgNP solution was increased up to 10×, the SERS intensity also increased because the larger number of AgNPs on the filter paper surface formed a SERS hot spot. However, when the AgNP solution concentration exceeded 10×, the aggregation of the AgNPs resulted in the decrease of the SERS intensity. Previous research [25] reported that the aggregation of nanoparticles in the vertical direction piled up the three-dimensional nanostructure and eliminated the SERS hot spot. Similar aggregation structures were also identified in the present study and are shown in Figure 8(e)–8(h).

3.1.3 Reproducibility and limit of detection of SERS measurement

The reproducibility of detection and limit of detection (LOD) are essential parameters for a molecule-detecting sensor. To determine the reproducibility of the SERS intensity, we measured the signals from 30 different AgNP spots that were formed by 2 μL of 10× concentrated AgNP solution. The 30 spots were treated with 1,000 nM of 4-ATP solution. Figure 10 shows the distribution of the SERS intensity that was acquired from the 30 different AgNP spots at the 1073 cm^{-1} band of 4-ATP. The relative standard deviation (RSD) of the total intensity was about 7.7%. The RSD in present study was slightly higher or similar to previous studies [19], [28] that evaluated the RSD of SERS intensity using 4-ATP. These studies applied the filtering and dipping methods with a higher amount of 4-ATP solution to treat the molecules on the SERS substrate. These filtering and dipping methods could have introduced more uniform adsorption of the molecules on the SERS substrate because the time for treatment was longer compared to the drop and dry method that was used in present study. Thus, considering the small amount of solution required in the present study, the simple drop and dry method combined with hydrophobic-treated filter paper showed good reproducibility of the SERS intensity.

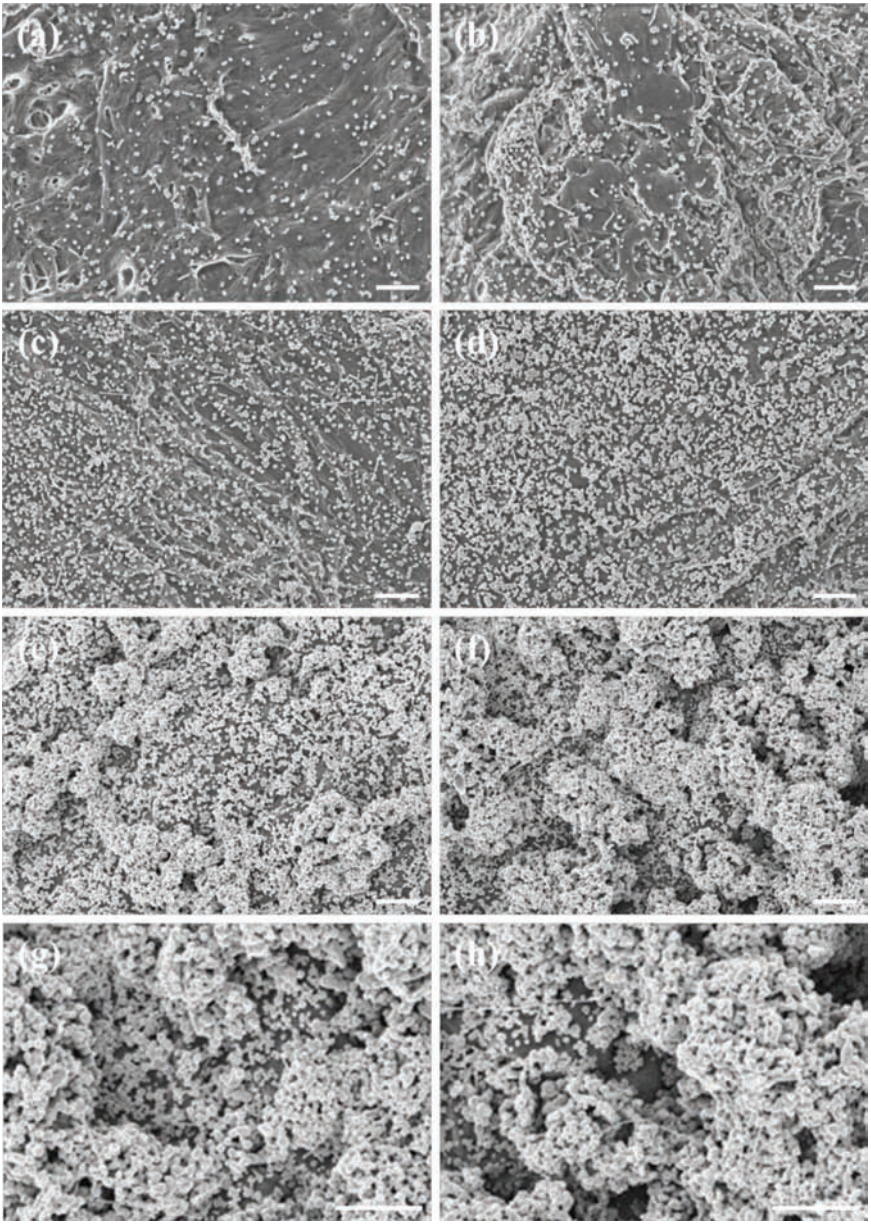

Figure 8. FE-SEM images of the AgNP solution droplet on the hydrophobic filter paper. AgNP solution concentration ratios of: (a) 1×, (b) 2×, (c) 5×, (d) 10× and (e) 20×. Panels (f), (g) and (h) show the 40× concentrated AgNP solution.

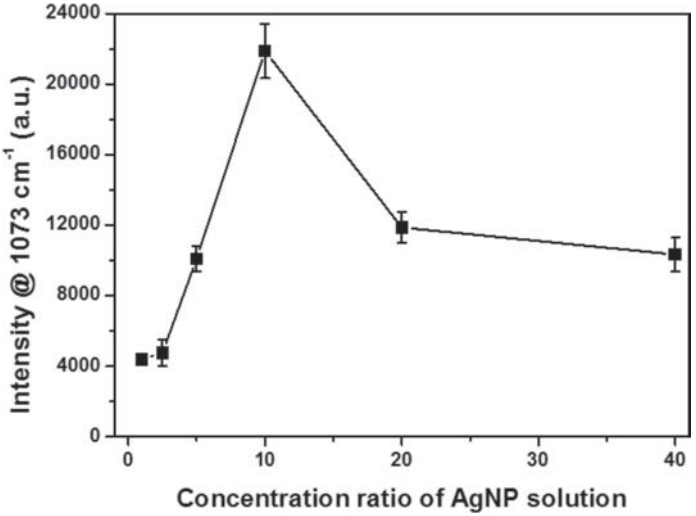

Figure 9. The SERS intensities of 4-ATP from different concentration ratios of the AgNP droplets on hydrophobic filter paper.

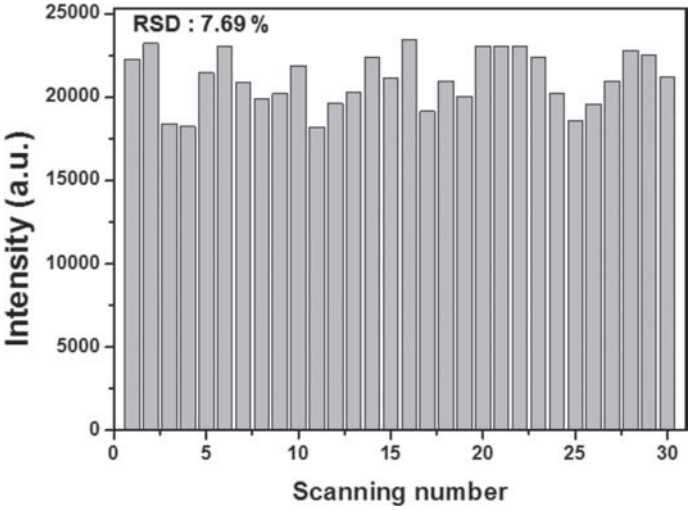

Figure 10. SERS intensity of 4-ATP on 30 different AgNP spots on hydrophobic filter paper.

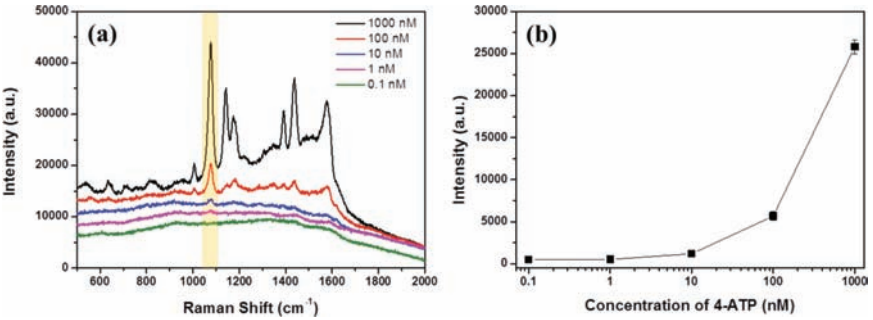

Figure 11. (a) The SERS spectra for different concentrations of 4-ATP. (b) The average SERS intensity at different concentrations of 4-ATP.

To determine the detection limit for 4-ATP on the hydrophobic-treated SERS substrate, a series of diluted 4-ATP solutions were applied at the AgNP spot on the SERS-active substrate. The 4-ATP solutions were diluted in water and ranged from 1000 nM to 0.1 nM. Figure 11(a) shows the Raman spectra for the different 4-ATP concentrations. The SERS intensity of the 1073 cm^{-1} band of the 4-ATP Raman peak was plotted against the 4-ATP concentration and is shown in Figure 11(b). The amount of the applied solution was 5 μL, and 4-ATP was detected at the femtomolar level using the hydrophobic-treated substrate. The RSD and the LOD suggest that the treated filter paper was not only a simple method but also a practical one.

3.1.4 Relationship between objective lens magnification and SERS intensity

The easiest way to increase the SERS intensity under the same conditions is to increase the magnification of the objective lens of the microscope. Figure 12 shows the relationship between increasing lens magnification and the SERS intensity of the 1073 cm^{-1} band of 4-ATP on the AgNP spots on the hydrophobic-treated filter paper. As the magnification of the objective lens increased, the SERS intensity gradually increased, but the reproducibility was decreased. The RSDs for magnifications of 10×, 20×, and 40× of the objective lenses were 5.8%, 9.7% and 15.8%, respectively. There was a limit to the achievable increase in SERS intensity from increasing the objective lens magnification.

The stronger SERS intensity with increased magnification of the objective lens could be explained by an increase in the numerical aperture (NA) of the lens. Table 1 shows the magnification and NA values of the objective lens used in this study along with the theoretical half angle (θ) value that was calculated using Eq. (1).

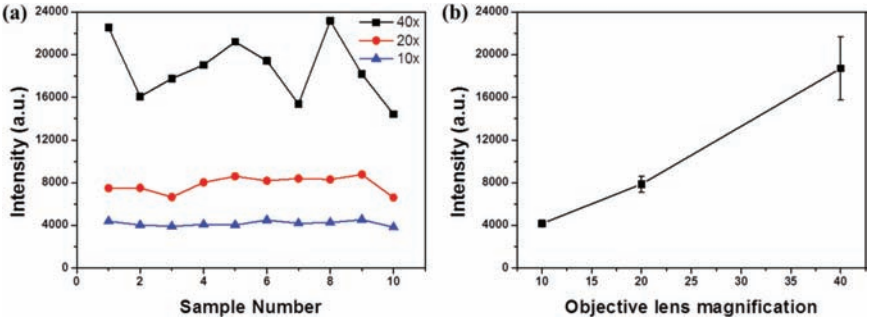

Figure 12. (a) SERS intensity of the 1073 cm^{-1} band of 4-ATP with different objective lens magnifications. (b) Summarized SERS intensity and standard deviations. Scanning size: 200 μm by 200 μm; step size: 1 μm; laser power: 0.4 mW; acquisition time: 2.5 sec.

Table 1. Numerical aperture and half angle dependence on the magnification of the objective lens

Magnification of objective lens	*Numerical aperture* (NA)	*θ*
10×	0.25	15.0 °
20×	0.40	24.0 °
40×	0.65	40.7 °

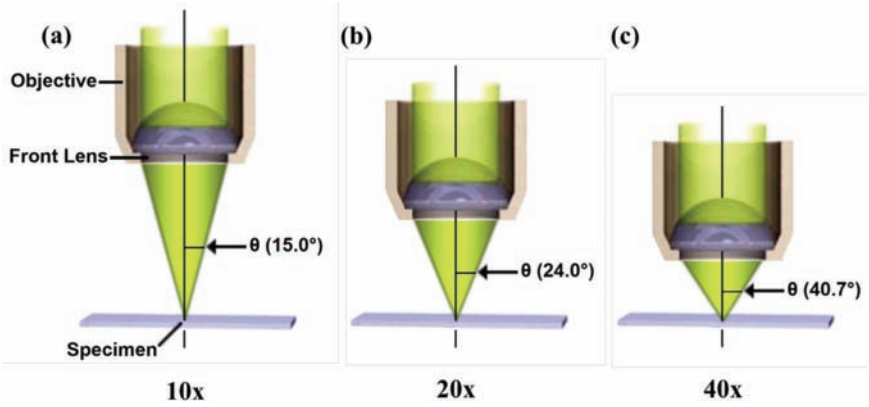

Figure 13. Theoretical effective scattering volume depending on the numerical aperture of the objective lens.

$$NA = n \sin \theta \quad (1)$$

Where n is the refractive index of air ($n = 1$), and θ is the half angle of incident light. In a high magnification lens (Figure 13), a strong SERS signal can be detected because the lens can accept wide-angle scattered light. As the magnification of the objective lens was increased, the uniformity of the SERS intensity was reduced because the signal intensity became sensitive to the height difference of the filter paper. Therefore, improvement of the surface uniformity of the filter paper can increase the SERS reproducibility and intensity because a high magnification lens can be used.

3.2 Cellulose nanofibrils coating for improving reproducibility of SERS intensity

3.2.1 CNF coating on hydrophobic-treated filter paper

We also tried to improve the sensor uniformity by applying a CNF coating to the hydrophobic-treated filter paper. The CNF coating was similar in chemical structure compared to the filter paper and thus was a suitable material for surface treatment. The small size of the CNF allows it to fill the pores of the filter paper and increase the surface smoothness. When the CNF coating was applied to the filter paper, a suspension containing 3 pph of CMC was used to control the penetration of the CNF into the filter paper. The small amount of the CMC suspension that increased the viscosity of the aqueous phase improved the retention of the CNF on the surface of the filter paper. Previous research [27] has shown that the addition of CMC improved the dispersing of CNF by disentangling the nanofibrils and increasing the anionic charge in the suspension. This dispersion of CNF resulted in the formation of a uniform surface. The PPS roughness of CNF coated filter paper is shown in Figure 14. The CNF coating slightly increased the roughness of the filter paper because the wetting and drying of the filter paper in CNF coating process caused nonuniform swelling and shrinking of the paper. The contact angle of the CNF coated filter paper slightly decreased with CNF coatings. The contact angle of the hydrophobic filter paper was about 114 °. When two CNF coatings were applied, the angle changed to 105 °. Even though the water contact angle slightly decreased, it was high enough to form AgNP spot on the paper surface. The coat weight of 1.2 g/m^2 was applied in each CNF coating.

3.2.2 Effect of CNF coating on the AgNP spot characteristics

The surface uniformity of the filter paper was improved by applying the CNF coating, as shown in Figure 15. Many large pores remained on the

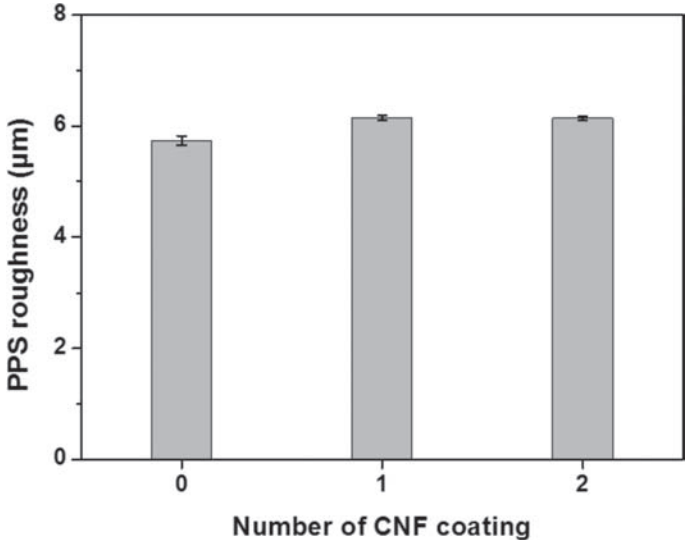

Figure 14. Roughness of the filter paper depended on number of CNF coatings.

hydrophobic-treated filter paper, as shown in Figure 15(a). The pores disappeared with the CNF coating because the pores were filled with CNF; surface smoothness was also improved (Figure 15(b) and 15(c)). The change of the filter paper surface affected on the shape and coverage of the AgNP spots (Figure 15(d), 15(e) and 15(f)). The rough outline of the AgNP spot was formed without CNF coating. The CNF coating, however, made the spot outline smooth by decreasing the roughness of the surface. The shape of the AgNP spot became more circular.

There were areas where the AgNPs were not loaded because of the differences in the heights and hydrophobic characteristics of the hydrophobic-treated papers. The AgNP solution did not penetrate into the deep pores in which there were no AgNPs (Figure 15(g)). Most areas, however, were covered by the AgNPs on the filter paper that was treated twice with the CNF coating. We used image analysis to evaluate seven different AgNP spots in each condition to analyse the coverage of the AgNPs. The coverage was gradually increased and the standard variation was decreased with the CNF coating (Figure 16). Thus, introducing a simple CNF coating made more uniform AgNP spots on the paper-based SERS substrate.

3.2.3 Reproducibility of SERS intensity with CNF coating

The reproducibility of SERS intensity was evaluated by applying 10,000 nM of a 4-ATP solution on the AgNP spot. The scanning condition was slightly changed

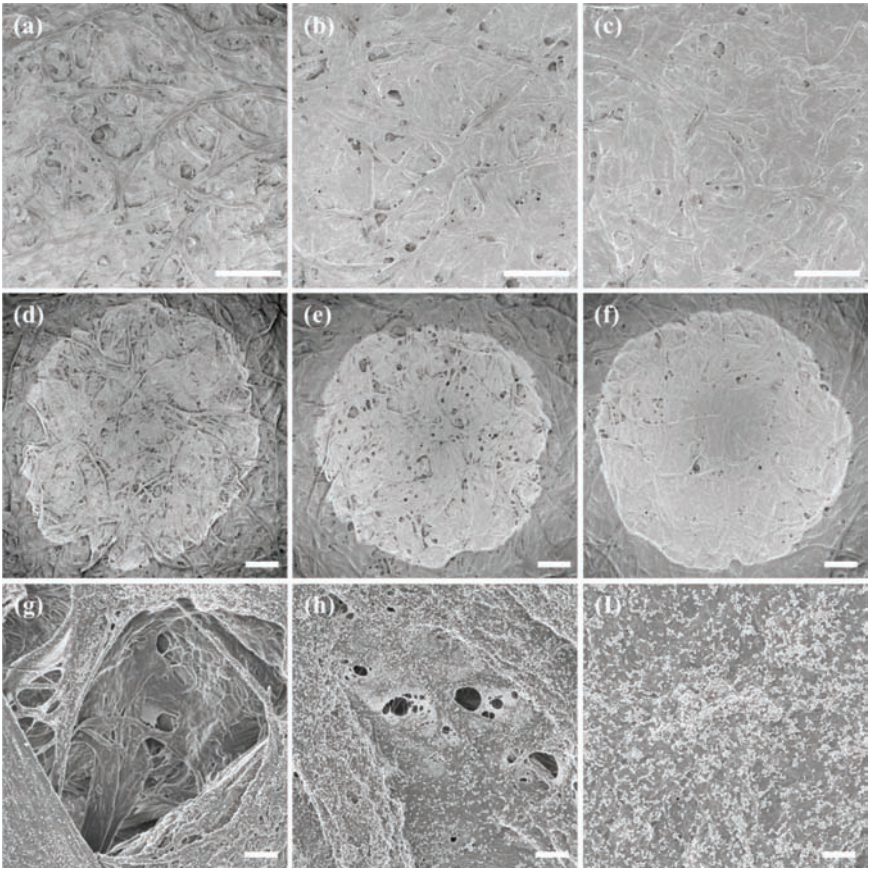

Figure 15. Surface changes of the filter paper as a result of the CNF coating. (a) CNF coating = 0, (b) CNF coating = 1 and (c) CNF coating = 2. Characteristics of the AgNP spot. (d) and (g) CNF coating = 0, (e) and (h) CNF coating = 1 and (f) and (l) CNF coating = 2. Scale bars in (a)–(f): 200 μm. Scale bars in (g)–(l): 2 μm.

because of the saturation of SERS intensity when the previous condition was applied. The scanning size, step size and laser power were 200 μm by 200 μm, 2 μm and 0.5 mW, respectively. The objective lens magnification was 40×. The scanning time was 0.625 sec. The SERS intensity of the 1073 cm^{-1} band of 4-ATP was increased by the CNF coating. The intensity was greatly increased when the CNF coating was applied once. The SERS intensity of the filter paper that was coated with CNF twice was similar when compared to filter paper that was coated once (Figure 17).

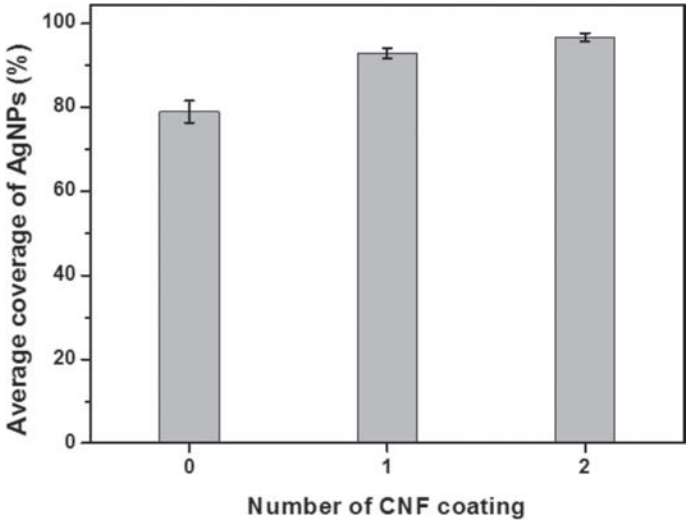

Figure 16. Coverage of the AgNP spot depended on the number of CNF coatings.

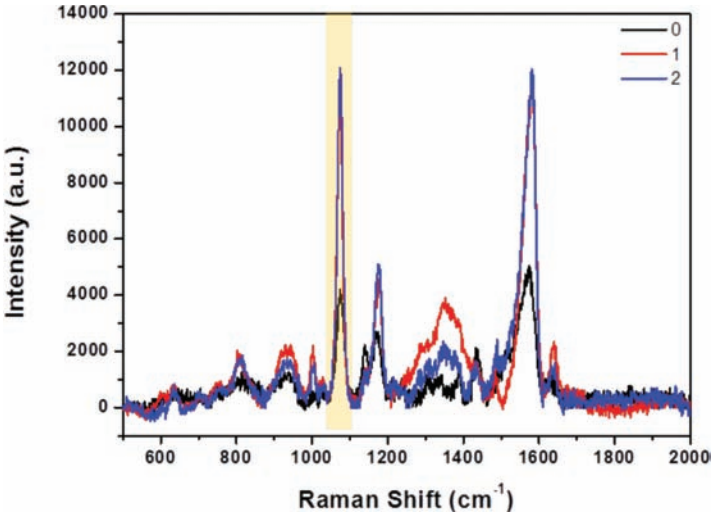

Figure 17. SERS intensity of 4-ATP depended on the number of CNF coatings.

Figure 18 shows the SERS intensity for the seven different AgNP spots in each condition. The summarised SERS intensities are given in Figure 18(d). The SERS intensity was increased by applying the CNF coating once; however, there was no difference between filter papers that were coated with CNF once or twice.

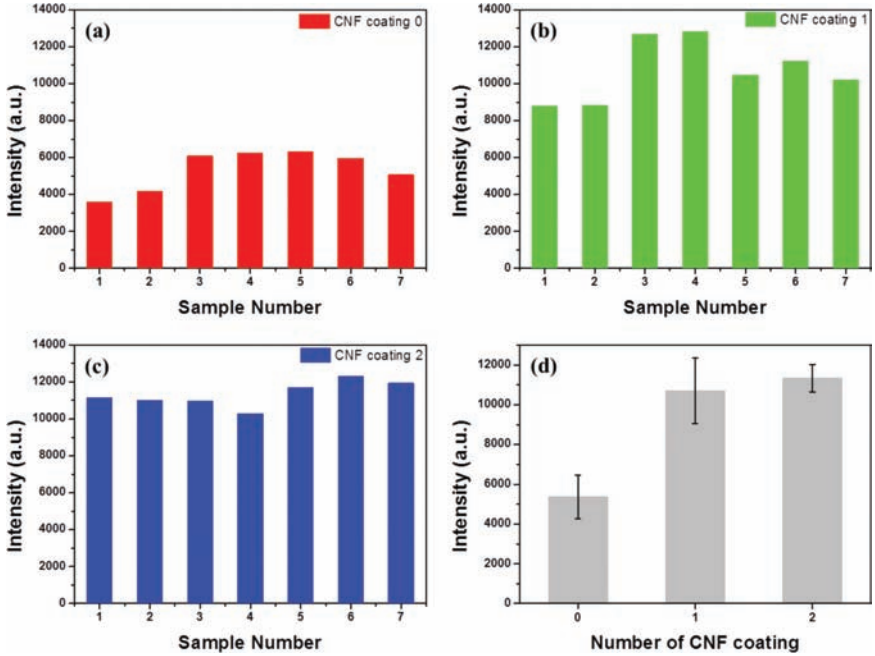

Figure 18. SERS intensity variation in the 1073 cm^{-1} band. (a) Hydrophobic-treated filter paper. (b) Application of one CNF coating. (c) Application of two CNF coatings. (d) Summarised SERS intensities and standard deviations.

The intensity was slightly increased, but the standard deviation was greatly decreased with additional CNF coatings. From these results, the RSD was calculated (Table 2). The RSD was decreased from 20% to 6% in the hydrophobic-treated filter paper with two CNF coatings. CNF coatings that filled the pores of the surface made more AgNPs retained on the paper surface, which increased the intensity of the SERS signal by forming the more SERS hot spot. CNF coatings also improved the uniform distribution of the AgNPs, which increased the reproducibility of the SERS signal. These results suggest that a simple CNF coating can greatly improve the reproducibility of SERS intensity even though a high magnification lens (40×) was used.

Table 2. Relative standard deviations of SERS intensity depending on the number of CNF coatings

Number of CNF coating	0	1	2
Relative standard deviation (%)	20.4	15.4	6.1

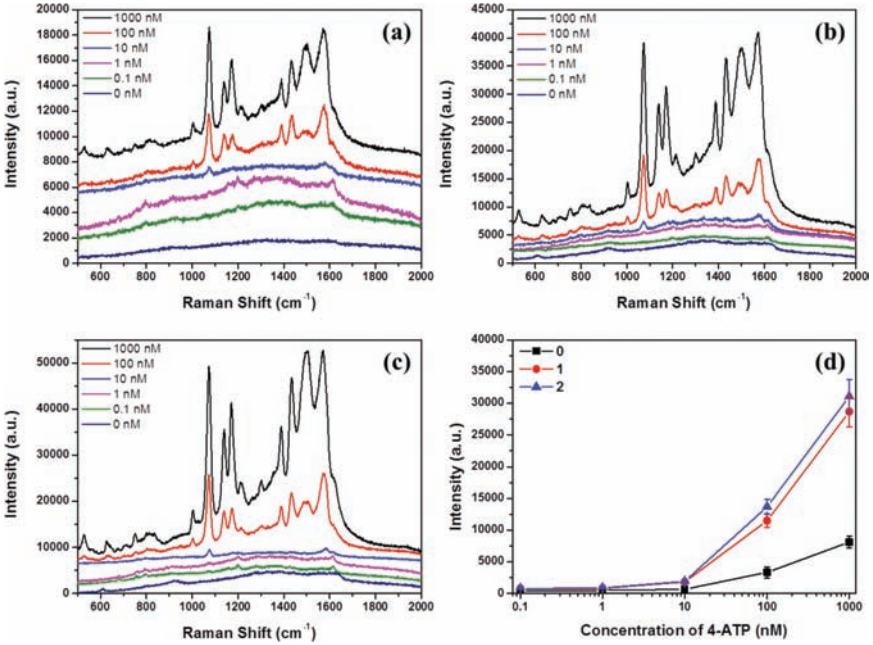

Figure 19. Limit of detection of 4-ATP depended on the number of CNF coatings. Scanning size: 200 μm by 200 μm; step size: 2 μm; laser power: 0.5 mW; acquisition time: 2.5 sec. (a) Hydrophobic filter paper (CNF coating = 0). (b) CNF coating = 1. (c) CNF coating = 2. (d) Average SERS intensity in 1073 cm^{-1} depending on 4-ATP concentration.

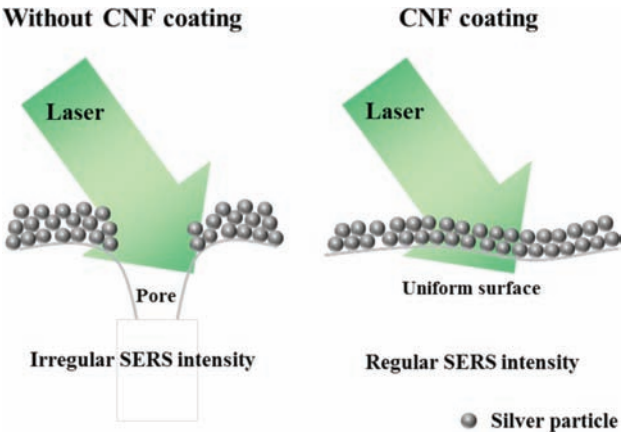

Figure 20. Schematic illustration of the CNF coating.

3.2.4 LOD dependency on the number of CNF coatings

The LOD of the 4-ATP molecule depended on the number of CNF coatings as shown in Figure 19. For all the substrates tested, the SERS intensity decreased with decreasing 4-ATP concentration. In the case of the CNF-untreated hydrophobic filter paper, the LOD was 10 nM; however, the LOD was improved by introducing the CNF coating. The LOD was 1 nM regardless of the number of CNF coatings. The uniform filter paper surface that was formed by the CNF coating made the intensity strong and improved the LOD. A schematic illustrating the application of a CNF coating is presented in Figure 20.

4 CONCLUSIONS

In this study, we fabricated a sensitive and uniform molecule-detecting sensor based on filter paper. The smoothness of the filter paper after hydrophobic treatment was improved through the calendaring process. The AgNP spots were formed using the drop and dry method to apply a AgNP solution of optimised concentration onto the surface of hydrophobic-treated filter paper. After the analyte was treated in the same manner on the AgNP spots, the molecule was detected using the SERS technique. We were able to detect trace amounts of 4-ATP at the femtomolar level using the filter paper with hydrophobic treatment, and we also confirmed that the paper showed high detection reproducibility through an area scanning application. To improve the reproducibility and intensity of the SERS signal, a CNF coating was applied to increase the uniformity of the filter paper surface. The CNF coating also improved the uniformity of the AgNP spots by reducing the paper pore size and increasing the surface smoothness. The improvements to the filter paper rendered by the CNF coating increased the intensity and reproducibility of the SERS signal even though an objective lens with high magnification was used.

REFERENCES

1. Y. H. Lai, S.-C. Kuo, Y.-C. Hsish, Y.-C. Tai, W.-H. Hung and U.-S. Jeng. Electrochemically fabricated gold dendrites with underpotential deposited silver monolayers for a bimetallic SERS-active substrate. *RSC Adv* **6**(16): 13185–13192, 2016.
2. E. Ko, J. Hwang, J. H. Kim, J. H. Lee, S.-H. Lee, V.-K. Tran, W. S. Chung, C. H. Park, J. Choo and G. H. Seong. Electrochemical fabrication of nanostructures on porous silicon for biochemical sensing platform. *Anal Sci* **32**(6): 681–686, 2016.
3. W. Ye, D. Wang, H. Zhang, F. Zhou and W. Liu. Electrochemical growth of flowerlike gold nanoparticles on polydopamine modified ITO glass for SERS application. *Electrochim Acta* **55**(6): 2004–2009, 2010.

4. S. B. Chaney, S. Shanmukh, R. A. Dluhy and Y.-P. Zhao. Aligned silver nanorod arrays produce high sensitivity surface-enhanced Raman spectroscopy substrate. *Appl Phys Lett* **87**(3): 031908, 2005.
5. S. Xu, B. Man, S. Jiang, J. Wang, J. Wei, S. Xu, H. Liu, S. Gao, H. Liu, Z. Li, H. Li and H. Qiu. Graphene/Cu nanoparticle hybrids fabricated by chemical vapour deposition as surface enhanced Raman scattering substrate for label-free detection of adenosine. *ACS Appl Mater Interfaces* **7**(20): 10977–10987, 2015.
6. N. A. Hatab, C.-H. Hsueh, A. L. Gaddis, S. T. Retterer, J.-H. Li, G. Eres, Z. Zhang and B. Gu. Free-standing optical gold bowtie nanoantenna with variable gap size for enhanced Raman spectroscopy. *Nano Lett* **10**(12): 4952–4955, 2010.
7. C. A'Andrea, J. Bochterle, A. Toma, C. Huck, F. Neubrech, E. Messina, B. Fazio, O. M. Marago, E. Di Fabrizio, M. Lamy De La Chapelle, P. G. Cucciardi and A. Pucci. Optical nanoantennas for multiband surface-enhanced infrared and Raman spectroscopy. *ACS Nano* **7**(4): 3522–3531, 2013.
8. A. Hakonen, M. Svedendahl, R. Ogier, Z.-J. Yang, K. Lodewijks, R. Verre, T. Shegai, P. O. Andersson and M. Käll. Dimer-on-mirror SERS substrates with attogram sensitivity fabricated by colloidal lithography. *Nanoscale* **7**(21): 9405–9410, 2015.
9. D. Zhu, H. Huang, G. Zhang, X. Li, X. Zhang. T. Wang and B. Yang. Fabrication of heterogeneous double-ring-like structure arrays by combination of colloidal lithography and controllable dewetting. *Langmuir* **28**(5): 2873–2880, 2012.
10. Y. H. Ngo, D. Li, G. P. Simon and G. Garnier. Gold nanoparticle-paper as a three-dimensional surface enhanced Raman scattering substrate. *Langmuir* **28**(23): 8782–8790, 2012.
11. C. H. Lee, M. E. Hankus, L. Tian, P. M. Pellegrino and S. Singamaneni. Highly sensitive surface enhanced Raman scattering substrates based on filter paper loaded with plasmonic nanostructures. *Anal Chem* **83**(23): 8953–8958, 2011.
12. C. H. Lee, L. Tian and S. Singamaneni. Paper-based SERS swab for rapid trace detection on real-world surfaces. *ACS Appl Mater Interfaces* **2**(12): 3429–3435, 2010.
13. C. Wang, B. Liu and X. Dou. Silver nanotriangles-loaded filter paper for ultrasensitive SERS detection application benefited by interspacing of sharp edges. *Sens Actuators B Chem* **231**: 357–364, 2016.
14. J. A. Webb, J. Aufrecht, C. Hungeford and R. Bardhan. Ultrasensitive analyte detection with plasmonic paper dipsticks and swabs integrated with branched nanoantennas. *J Mater Chem C* **2**(48): 10446–10454, 2014.
15. K. Zhang, J. Zhao, H. Xu, Y. Li, J. Ji and B. Liu. Multifunctional paper strip based on self-assembled interfacial plasmonic nanoparticle arrays for sensitive SERS detection. *ACS Appl Mater Interfaces* **7**(30): 16767–16774, 2015.
16. W. W. Yu and I. M. White. A simple filter-based approach to surface enhanced Raman spectroscopy for trace chemical detection. *Analyst* **137**(5): 1168–1173, 2012.
17. E. P. Hoppmann, W. W. Yu and I. M. White. Highly sensitive and flexible inkjet printed SERS sensors on paper. *Methods* **63**(3): 219–224, 2013.
18. W. W. Yu and I. M. White. Inkjet printed surface enhanced Raman spectroscopy array on cellulose paper. *Anal Chem* **82**(23): 9626–9630, 2010.

19. Y. Li, K. Zhang, J. Zhao, J. Ji, C. Ji and B. Liu. A three-dimensional silver nanoparticles decorated plasmonic paper strip for SERS detection of low-abundance molecules. *Talanta* **147**(15): 493–500, 2016.
20. C. Desmonda, S. Kar and Y. Tai. Formation of gold nanostructures on copier paper surface for cost effective SERS active substrate – Effect of halide additives. *Appl Surf Sci* **367**(30): 362–369, 2016.
21. L. R. Arcot, K. M. A. Uddin, X. Chen, X. Wenchao, K. Xianming, L. S. Johansson, R. H. A. Ras and O. J. Rojas. Paper-based plasmon-enhanced protein sensing by controlled nucleation of silver nanoparticles on cellulose. *Cellulose* **22**(6): 4027–4034, 2015.
22. Y. Meng, X. Jiang, Q. Zhao and J. Zhan. Silver nanoparticles decorated filter paper via self-sacrificing reduction for membrane extraction surface-enhanced Raman spectroscopy detection. *Analyst* **138**(7): 2090–2095.
23. M.-L. Cheng, B. C. Tsai and J. Yang. Silver nanoparticle-treated filter paper as a highly sensitive surface-enhanced Raman scattering (SERS) substrate for detection of tyrosine in aqueous solution. *Anal Chim Acta* **708**(1–2): 89–96, 2011.
24. H. Chang, H. Kang, S. Jeong, E. Ko, Y.-S. Lee, H.-Y. Lee and D. H. Jeong. A fast and reliable readout method for quantitative analysis of surface-enhanced Raman scattering nanoprobes on chip surface. *Rev Sci Instrum* **86**(5): 055004, 2015.
25. L. Zhang, C. Guan, Y. Wang and J. Liao. Highly effective and uniform SERS substrates fabricated by etching multi-layered gold nanoparticle arrays. *Nanoscale* **8**(11): 5928–5937, 2016.
26. C.-C. Yu, S.-Y. Chou, Y.-C. Tseng, S.-C. Tseng, Y.-T. Yen and H.-L. Chen. Single-shot laser treatment provides quasi-three-dimensional paper-based substrates for SERS with attomolar sensitivity. *Nanoscale* **7**(5): 1667–1677, 2015.
27. V. Kumar, A. Elfving, H. Koivula, D. Bousfield and M. Toivakka. Roll-to-roll processed cellulose nanofiber coatings. *Ind Eng Chem Res* **55**(12): 3603–3613, 2016.
28. Y.-E. Shi, M. Yang, X. Jiang, Q. Zhao and J. Zhan. A disordered silver nanowires membrane for extraction and surface-enhanced Raman spectroscopy detection. *Analyst* **139**(10): 2525–2530, 2014.
29. P. C. Lee and D. Meisel. Adsorption and surface-enhanced Raman of dyes on silver and gold sols. *J Phys Chem* **86**(17): 3391–3395, 1982.

Transcription of Discussion

PAPER-BASED CHEMICAL DETECTING SENSORS FOR SURFACE-ENHANCED RAMAN SCATTERING

Kyudeok Oh,[1,2] *Minwoo Lee,*[3] *Hye Jung Youn,*[1,2] *Dae Hong Jeong*[3] *and Hak Lae Lee*[1,2]

[1] Department of Forest Sciences, College of Agriculture and Life Sciences, Seoul National University
[2] Research Institute of Agriculture and Life Sciences, Seoul National University
[3] Department of Chemistry Educations, College of Education, Seoul National University

Vikram Singh Raghuwanshi Monash University

I have a question on the production of silver nanoparticles. How do you control the shape and size of silver nanoparticles when you produce them?

Hak Lae Lee Seoul National University

First of all, we have to control the temperature of the silver nitrate solution and also try controlling the starting conditions. They are the only two things, and also we use silver citrate as a dispersant with stabilizers, so we needed to control the amount of stabilizers applied.

Gil Garnier Monash University

I have a few questions on that because I presented on the topic at the last conference in Cambridge, and I know a little bit about this. Why do you use sized paper?

Discussion

Hak Lae Lee

As you see here, unsized paper will suck in all the nanoparticles into the internal structures, so we needed to keep the nanoparticles on the surface – and nano particles do not spread in the X–Y directions, either. We needed to keep the nanoparticles congested in a small area, so we applied sizing to keep the droplets to a small size.

Gil Garnier

Did you compare with unsized paper?

Hak Lae Lee

Yes, of course.

Gil Garnier

What did you achieve?

Hak Lae Lee

Unsized paper did not give any strong SERS intensities at all.

Gil Garnier

Your results contradict our studies. We found that at constant nanoparticle loading, SERS intensity on unsized paper is much higher than on sized paper. This is because of the 3D-distribution of particles provided hotspots. So now my second question will be on the distribution, I saw on your very interesting presentation that it was sometime a little bit on the curvy side. So the question is, have you done reproducibility experiments? If you take a sample and you do 10 measurements, how much variability do you have in terms of intensity?

Hak Lae Lee

I have shown in one of my slides that reproducibility is quite important and our case is 6.2%, which is quite low, and it is quite important to keep the molecules on the surface. For that we needed to have more close-packed nanoparticles on the surface.

Gil Garnier

Why did you choose to use so big nanoparticles? The nanoparticles are 100 nm and typically in SERS research we use between 4 and 25, why did you go for this extreme range?

Hak Lae Lee

The particle size you mean? We used, an average particle size of the nanoparticles of 90 nm and it does not matter if you have a smaller than the wavelength of your laser light.

Gil Garnier

Have you tried lower size?

Hak Lae Lee

No, we did not.

Gil Garnier

Because typically well-distributed small nano partially create hotspots, which are a function of the number of contacts. Therefore, the smaller the particle, the more contact, the more hotspots, the more amplification.

Hak Lae Lee

We did not change the particle size yet, so this work just showed the impact of the paper substrate**.** That is a good topic to pursue.

Gil Garnier

The last question that I would like to ask is have you tried other SERS probes than ATP and aromatic molecule? Have you tried nonaromatic smaller linear molecules without phenyl groups?

Hak Lae Lee

No, we have not tried yet. We were focusing here on the effect of paper substrate.

Discussion

Gil Garnier

Yes, for the nanocellulose study you have achieved a beautiful result, you have a very smooth baseline and the peaks are decent. And your interpretation of that was the smoothness of the fiber. Have you looked at the nanoparticle distribution? The nano particle distribution of the Z direction, to see if they are more uniformly distributed?

Hak Lae Lee

We tried to keep the nanoparticles well distributed in the X–Y direction, only. Because, when you have stacking of the nanoparticles, you know the laser beam will not penetrate deeply.

Gil Garnier

Have you tried? Because what we have found is that the laser indeed goes very deep in the paper and you have the hotspot in the two layers of nanoparticle that interacts with the each other and that really increases the signal, so what are you doing if you have the more uniform distribution?

Hak Lae Lee

When you increase the saturation of the nanoparticles, they give you some more agglomerates which is almost like stacking of the nanoparticles. It gives lower intensities.

Gil Garnier

So you are now talking about aggregate size which is giving you a lot of hotspots.

Hak Lae Lee

That's true. But the ratio of molecules in hot spot decreases at the same time.

Thierry Mayade Ahlstrom-Munksjo Apprieu

As I understand it, you take a sheet of paper but you have to treat it, to size it, to calender it. What will be the interest or the limitation of using readily available parchment paper which is made of pure cellulose?

Hak Lae Lee

This is a good idea. You know we used a filter paper because it is a quite pure chemically, and also you can use some other substrate which is quite pure and smooth. And right now we are trying to work out what happens when you use CNF papers rather than filter paper, prepared form CNF only. So it is almost like parchment paper, I would say it gives a very smooth surface in the beginning without any pores, so I hope that gives some advantages. And I think parchment paper can be used too.